





## A new species of the genus *Dysommima* (Teleostei: Anguilliformes: Synphobranchidae: Ilyophinae) from the eastern Indian Ocean

KENNETH A. TIGHE<sup>1,\*</sup> & JOHN J. POGONOSKI<sup>2</sup>

<sup>1</sup>Department of Vertebrate Zoology, National Museum of Natural History, Smithsonian Institution, Museum Support Center, MRC 534, 4210 Silver Hill Road, Suitland, MD 20746, USA

 [tighek@si.edu](mailto:tighek@si.edu);  <https://orcid.org/0000-0003-1127-0949>

<sup>2</sup>CSIRO National Research Collections Australia, Australian National Fish Collection, GPO Box 1538, Hobart, TAS 7001, AUSTRALIA

 [john.pogonoski@csiro.au](mailto:john.pogonoski@csiro.au);  <https://orcid.org/0000-0002-4878-3919>

\*Corresponding author

### Abstract

*Dysommima pygmaea*, a new species of ilyophine eel from off Western Australia is described and illustrated. The species is distinguished from the other three species in the genus, *D. rugosa*, *D. orientalis*, and *D. brevis* by a lower number of total vertebrae, a higher number of predorsal vertebrae, coloration, and a smaller adult size.

**Key words:** Pisces, Elopomorphs, taxonomy, Australia, *Dysommima rugosa*

### Introduction

The genus *Dysommima* and its only included species, *D. rugosa*, was described by Ginsburg (1951) based on a single specimen (USNM 131594) taken off Cumberland Island, Georgia, in the western North Atlantic. Since the original description, *D. rugosa* has been reported to be widely distributed in the western North Atlantic, from off the Carolinas to the Gulf of Mexico and the Caribbean Sea, by Robins and Robins (1989). The species has also been reported from off Surinam (Uyeno & Sasaki 1983), off southern Brazil (Haimovici *et al.* 1994), off Angola (Tweddle & Anderson 2008), in the Mozambique Channel (Karrer 1983), Taiwan (Chen & Mok 2001; Ho *et al.* 2015), Japan (Hatoaka 1997), Vailulu'u Seamount (Staudigel *et al.* 2006) and Hawaii (Robins & Robins 1976). Recently, Tighe *et al.* (2018) described a new species, *D. orientalis*, based on the specimens previously reported from Taiwan and Japan. Vo *et al.* (2024) described a third species, *D. brevis*, from specimens collected in the South China Sea off the southeast coast of Vietnam. Recent collecting in the Indian Ocean off Western Australia yielded four specimens of an undescribed species in this genus.

### Materials and methods

General methods for morphometric and meristic data for this study are given in Böhlke (1989). Measurements over 100 mm were made with a 450 mm ruler to the nearest 1 mm and measurements between 10–100 mm were made with a digital caliper to the nearest 0.1 mm. Measurements under 10 mm were taken with an ocular micrometer to the nearest 0.1 mm. All measurements are given as a proportion of the total length (TL) except for subunits of the head which are presented as proportions of the head length (HL). Vertebral and fin-ray counts were taken from radiographs. Total vertebral counts are of all elements including the hypural plate. Preanal and predorsal vertebral counts were taken using the definitions of Böhlke (1982). The number of dorsal rays anterior to the anal origin are counted back to vertical through the first anal ray base. Cyanine blue was used for staining cephalic sensory pores (Saruwatari *et al.*, 1997). The holotype and one paratype (USNM 443847) were scanned on a GE Phoenix v|tome|x M 240/180kV Dual Tube  $\mu$ CT scanner at the Micro Computed Tomography Imaging Center

(mCTIC) at the Smithsonian Institution National Museum of Natural History Scientific Imaging Core Facility (RRID:SCR\_025090) with the following settings: 90 kV, 110  $\mu$ A, 250 ms exposure time, and 9.00258  $\mu$ m voxel size. The resulting x-ray projections were reconstructed into three-dimensional image stacks using the software package datos|x reconstruction vers. 2.4.0, and were visualized and segmented using 3D Slicer vers. 5.6.2 (Fedorov *et al.*, 2012). The resulting three-dimensional image stacks were uploaded to MorphoSource (media identification numbers 000768036 and 000768077, respectively). The type specimens are deposited at the National Museum of Victoria (NMV), the Australia National Fish Collection (CSIRO) and the United States National Museum of Natural History, Smithsonian Institution (USNM). Other institutional codes used follow Sabaj (2020; 2025).

***Dysommima pygmaea* sp. nov.**

Figures 1–13, Table 1

**Holotype:** NMV A 29681-004 (adult male, 145 mm TL); Australia: Western Australia: Rowley Shoals, Mermaid L34 east transect (17°02'50"S, 119°39'41"E to 17°03'42"S, 119°41'22"E), RV *Southern Surveyor*, Station SS0507/77, depth 424–456 m, captured with beam trawl, 18 June 2007.

A



B



**FIGURE 1.** Holotype of *Dysommima pygmaea*, NMV A 29681-004, 145 mm TL; Australia: Western Australia: Rowley Shoals. A. Immediately after capture. B. After preservation.

**Paratypes:** NMV A 29681-009 (169 mm TL, cleared and stained), CSIRO H 6607-01 (adult female, 147 mm TL), USNM 443847 (adult female, 161 mm TL); all collected with holotype.

**Diagnosis.** A species of the genus *Dysommima* with the following combination of characters: predorsal vertebrae 16, preanal vertebrae 27–28, total vertebrae 122, eye diameter about 12–14% head length, vomerine dentition four large compound teeth set in papillose pads, maxillary and mandibular teeth numerous but small.

**Description.** Body moderately elongate, slightly compressed in head and trunk. Pectoral fin present; dorsal-fin origin behind tip of pectoral fin; anal-fin origin approximately one head length behind pectoral-fin base. Snout projects very slightly beyond tip of lower jaw. Snout plicate, with four main plicae on each side of midline; median first plica L-shaped, extending laterally in front of second plica; second plica curves slightly laterally behind dorsal end of third plica, third and fourth plica smaller and less distinct than others; first supraorbital pore just above dorsal end of second and third plicae. Tip of lower jaw also plicate, with total of 12 plicae although only 8 extend outside of lip onto tip of jaw; two median plicae largest; three lateral plicae on each side of median plicae, reducing slightly in size from interior to exterior; first preopercular-mandibular pore just behind posterior end of third and fourth plicae. Anterior portion of snout and lower jaw extensively covered with papillae; papillae reduced in number posteriorly along head.

Morphometrics: Table 1 gives the summary of morphometrics for the type series. Morphometrics of the holotype: total length (TL) 145 mm, predorsal length 31.0 mm (21.4% TL), preanal length 42.9 mm (29.6% TL), tail length 102 mm (70.3% TL), trunk length 22.0 mm (15.2% TL), body depth (at gill opening) 10.2 mm (7.0% TL), body depth (at anal origin) 10.0 mm (6.9% TL), head length (HL) 20.8 mm (14.3% TL), eye diameter 2.6 mm (12.5% HL), interorbital width 4.0 mm (19.2% HL), snout length 5.7 mm (27.4% HL), upper jaw length 7.5 mm (36.1% HL), lower jaw length 7.2 mm (34.6% HL), pectoral fin length 4.6 mm (22.1% HL).

**TABLE 1.** Morphometric and meristic data of *Dysommia pygmaea*, *D. rugosa*, *D. orientalis* and *D. brevis*. For bilateral pore counts, the counts are recorded left/right.

Species	<i>D. pygmaea</i>		<i>D. rugosa</i>	<i>D. orientalis</i>	<i>D. brevis</i> *
	Holotype	Paratypes	Study Material	Study Material	Holotype, Paratype
Total length (mm)	145	147–169 (n=3) Mean (range)	96–347 (n=45) Mean (range)	238–625 (n=7) Mean (range)	319, 282
<b>% TL</b>					
Predorsal length	21.4	21.2 (20.7–21.7)	18.4 (15.3–21.1)	15.0 (14.0–16.2)	17.0, 17.7
Preanal length	29.6	28.7 (27.2–29.6)	28.9 (26.1–32.0)	28.7 (27.0–29.8)	24.6, 25.6
Tail length	70.3	70.9 (69.3–73.7)	70.9 (68.0–73.9)	71.1 (70.2–73.0)	75.4, 74.4
Trunk length	15.2	13.6 (13.0–14.8)	14.9 (11.7–17.2)	15.8 (14.2–17.6)	11.1, 11.8
Head length	14.3	14.4 (13.6–14.9)	14.1 (13.0–16.6)	13.2 (12.6–15.0)	13.5, 13.8
Depth at gill opening	7.0	6.4 (6.2–6.7)	5.6 (4.3–7.5)	5.2 (4.9–5.3)	5.7, 5.0
Depth at anus	6.9	6.9 (6.0–8.1)	5.6 (3.9–7.5)	4.7 (3.7–5.9)	5.9, 4.7
<b>% HL</b>					
Eye diameter	12.5	13.0 (12.3–13.6)	11.4 (9.7–15.3)	8.7 (7.6–9.8)	11.8, 12.3
Interorbital width	19.2	19.1 (18.8–19.3)	19.9 (12.6–23.5)	18.5 (17.1–19.5)	17.4, 15.9
Snout length	27.4	26.4 (25.5–27.4)	30.9 (24.6–37.7)	25.3 (23.2–27.8)	28.3, 28.5
Upper jaw length	36.1	36.3 (34.4–37.5)	44.3 (37.6–52.8)	45.9 (43.9–48.0)	43.6, 42.6
Lower jaw length	34.6	33.7 (32.4–35.1)	41.1 (33.3–49.7)	41.3 (39.0–43.4)	38.1, 36.7
Pectoral fin length	22.1	21.6 (19.8–22.6)	17.8 (13.3–23.3)	20.3 (16.8–23.4)	21.3, 18.5
<b>Vertebrae</b>					
Predorsal	16	16–16	13–16	11–12	12, 13
Preanal	28	27–27	28–31	26–32	23, 25
Precaudal	55		-	-	-
Total	122	122–122	123–132	137–141	134, 133
<b>Lateralis system</b>					
Cephalic pores					
Supraorbital	3/3	3/3	3/3	3/3	3/3, 3/3
Infraorbital	4/4	4/4	4/4	4/4	4/4, 4/4
Adnasal	1/1	1/1	1/1	1/1	0/0, 0/0
Preoperculomandibular	6/6	6/6	6/6	6/6	6/6, 6/6
Lateral line pores	Absent	Absent	Absent	Absent	Absent
<b>Fin rays</b>					
Dorsal-fin rays	289	271–300	286–339	304–321	338, 344
Anal-fin rays	244	258–276	251–307	260–289	304, 309
Anal fin origin below DR	34	29–34	36–57	51–60	42, 41
Pectoral fin rays	13	13–15	14–16	-	-
Caudal fin rays	15	15	13–15	-	-

.....continued on the next page

TABLE 1. (Continued)

Species	<i>D. pygmaea</i>		<i>D. rugosa</i>	<i>D. orientalis</i>	<i>D. brevis</i> *
	Holotype	Paratypes	Study Material	Study Material	Holotype, Paratype
<b>Dentition</b>					
Mandibular tooth rows	5–6	5–6	6–7	5–7	6, 6
Mandibular teeth (inner row)	29	28–30	39–51	44–50	44, 46
Maxillary tooth rows	5–6	5–6	7–8	6–8	5, 4
Maxillary teeth (inner row)	42	37–40	49–62	50–60	28, 29
Intermaxillary teeth	0	0	0	0	0
Vomerine teeth	4	4	4–5	3–4 large + 0–1 small	3+2, 4+1

\*Data from Vo *et al.* (2024)

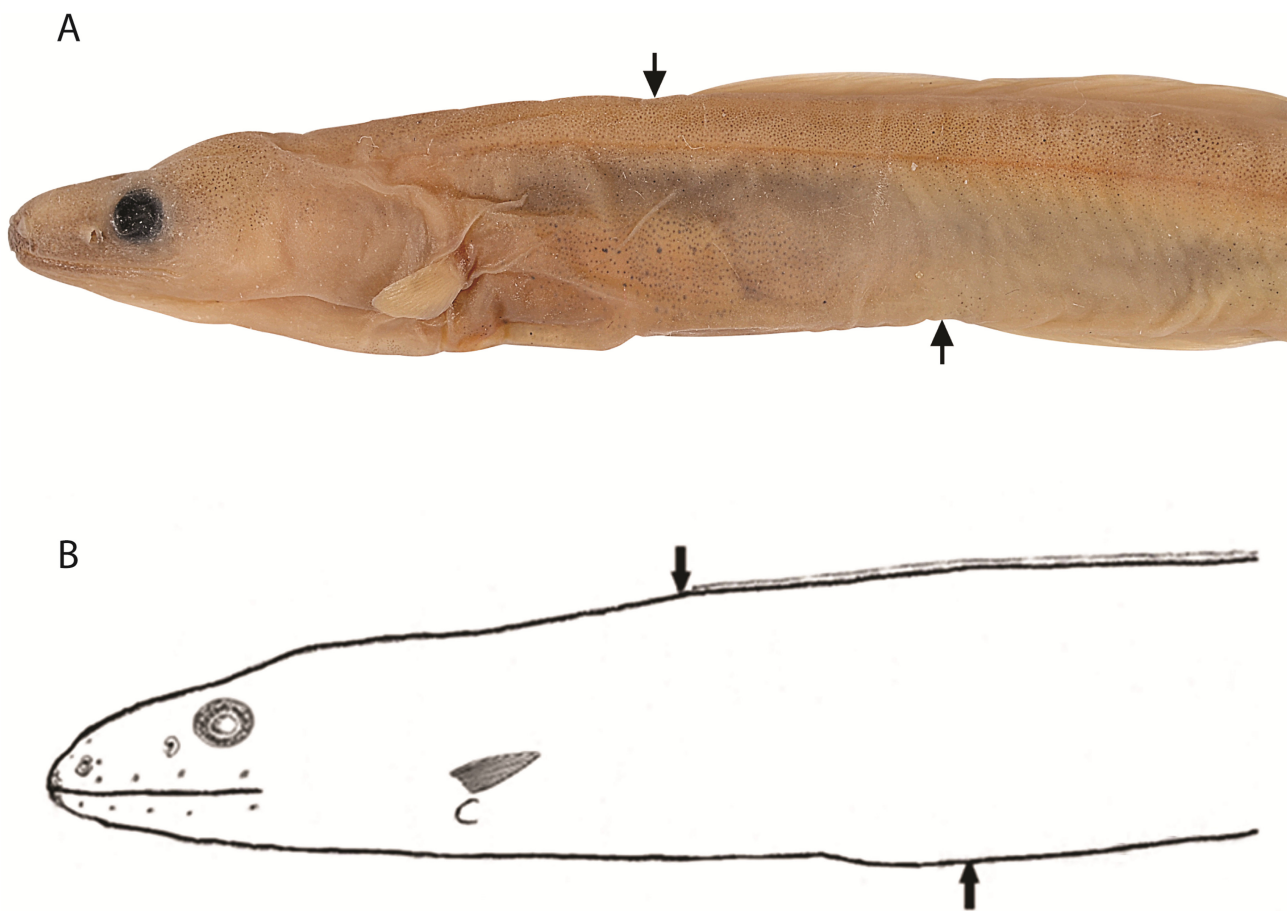


FIGURE 2. Holotype of *Dysommima pygmaea*, NMV A 29681-004. A. Lateral view of head and trunk. Arrows show dorsal and anal fin origins. B. Semi-diagrammatic illustration of lateral view of head showing cephalic pores.

Meristics: Table 1 gives the summary of meristics for the type series. Total vertebrae 122, predorsal vertebrae 16, preanal vertebrae 27–28. Dorsal rays 271–300, anal rays 244–276, anal fin origin at dorsal ray 29–34, pectoral rays 13–15 (based on cleared and stained paratype and CT scanned specimens), caudal rays 15.

Coloration: Live coloration (Figure 1A): body medium brown with irregular blotching on body slightly darker, head and area of gill opening very dark (probably from poor exposure of photograph since there is no concentration of melanophores in these areas after preservation), gut cavity slightly darker, overlain with iridophores producing a greenish silver sheen, fins very light and almost unpigmented. Coloration after preservation (Figure 1B): body



overall light tan, dotted with numerous small melanophores, gut cavity with slightly fewer but larger melanophores, internal gut cavity darker due to peritoneal pigmentation, two pairs of deep mid-lateral pigment spots near vertebrae 57–59 and 63–65 (probably representing remnants of larval pigment), fins light with little pigment.

Cephalic-lateralis pores (Fig. 2B): supraorbital 3; adnasal 1, infraorbital 4, preoperculo-mandibular 6. Lateral-line pores absent.

Dentition (Figs. 3–6). Intermaxillary teeth absent. Four relatively large, compound vomerine teeth (Figs. 3–4) set in papillose pads, fourth usually slightly smaller than the first three teeth on the palate. Mandibular teeth (Fig. 5) set in a band composed of 5–6 irregular rows anteriorly and decreasing gradually to 3–4 rows posteriorly, teeth increasing in size gradually from outer to inner with approximately 28–30 teeth in inner row. Maxillary teeth similar (Fig. 6) but set in a band composed of 5–6 irregular rows anteriorly and decreasing gradually to 2–3 rows posteriorly, teeth increasing in size gradually from outer to inner row with approximately 37–42 teeth in inner row.



**FIGURE 3.** Radiograph of anterior portion of holotype of *Dysommima pygmaea*, NMV A 29681-004. Arrows show dorsal and anal fin origins.



**FIGURE 4.** MicroCT scan of the skull of holotype of *Dysommima pygmaea*, NMV A 29681-004, ventral view showing the vomerine teeth.

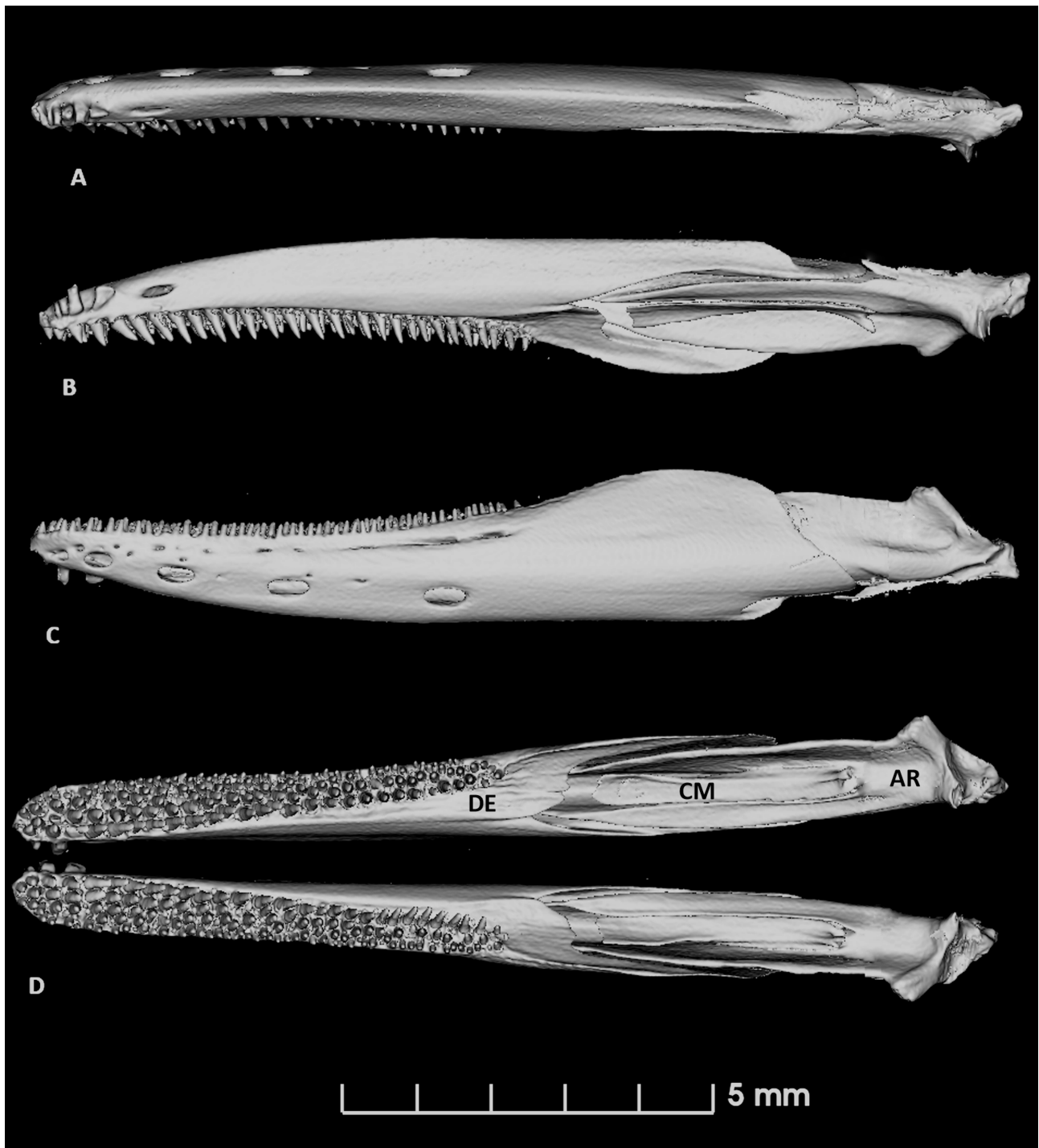


**FIGURE 5.** MicroCT scan of the mandible of holotype of *Dysommia pygmaea*, NMV A 29681-004. A. Ventral view of left mandible. B. Medial view of left mandible. C. Lateral view of left mandible. D. Dorsal view of entire mandibles. Abbreviations: AR, articular; CM, coronomeckelian ossification; DE, dentary.

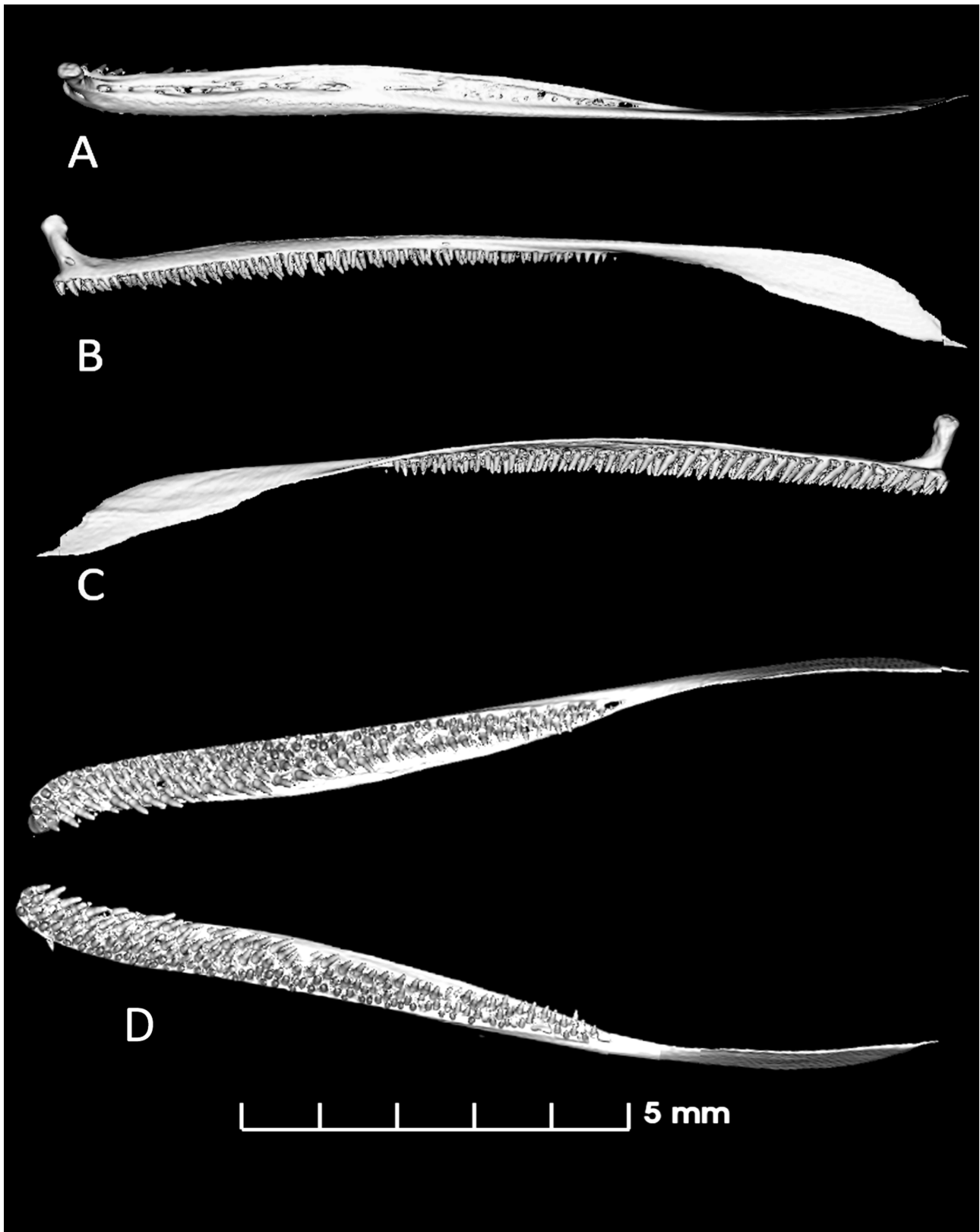


**FIGURE 6.** MicroCT scan of the maxilla of holotype of *Dysommima pygmaea*, NMV A 29681-004. A. Dorsal view of left maxilla. B. Lateral view of left maxilla. C. Medial view of left maxilla. D. Ventral view of both maxillae.

Osteology (Figs. 7–12). The osteology of *Dysommima pygmaea* is nearly identical to that of *D. rugosa* described by Robins and Robins (1970). Fig. 7 shows the osteology of the head of *D. pygmaea* in dorsal, lateral and ventral views. Details of the osteology are discussed individually in the sections below.

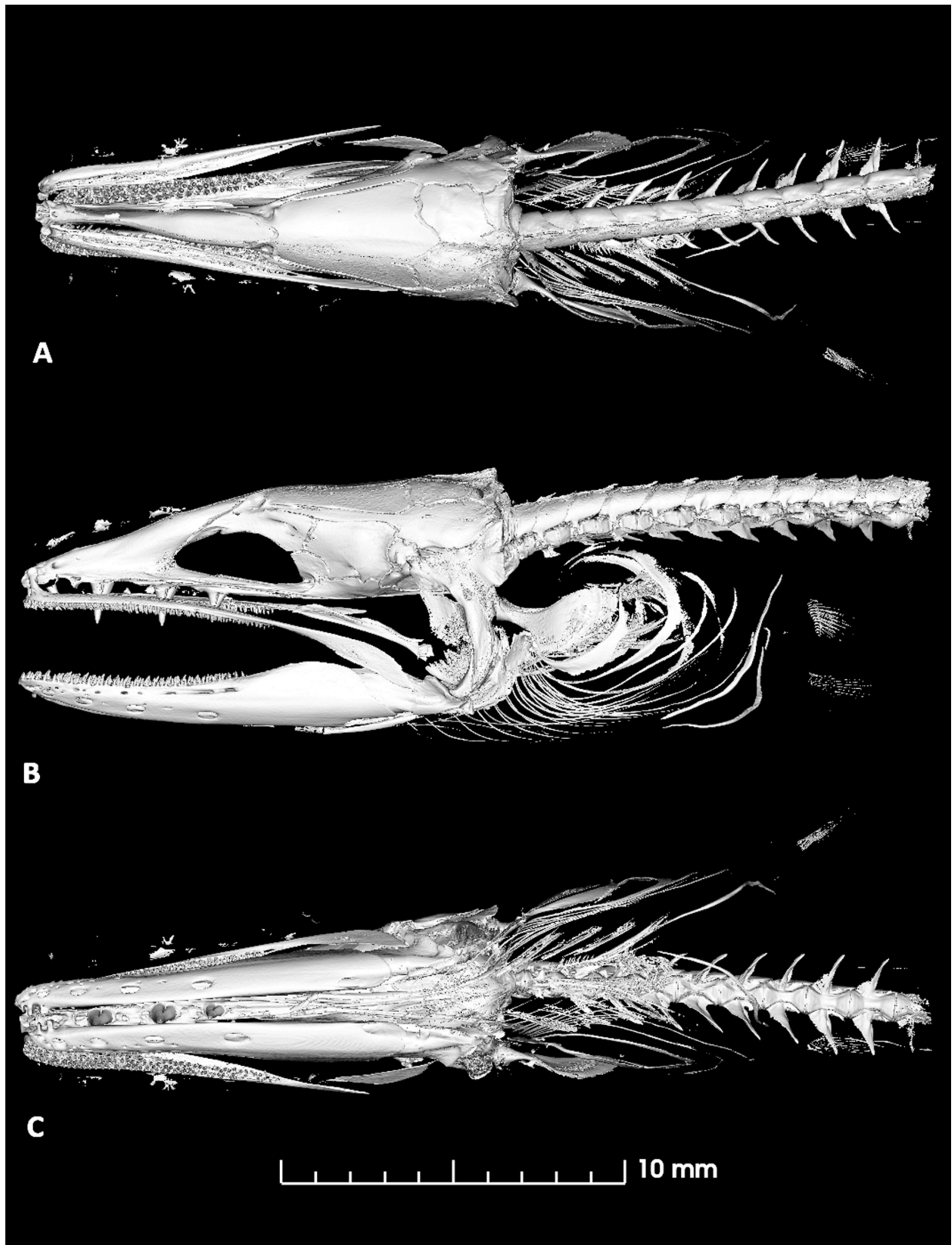


**FIGURE 7.** MicroCT scan of the anterior portion of holotype of *Dysommima pygmaea*, NMV A 29681-004. A. Dorsal view. B. Lateral view. C. Ventral view.

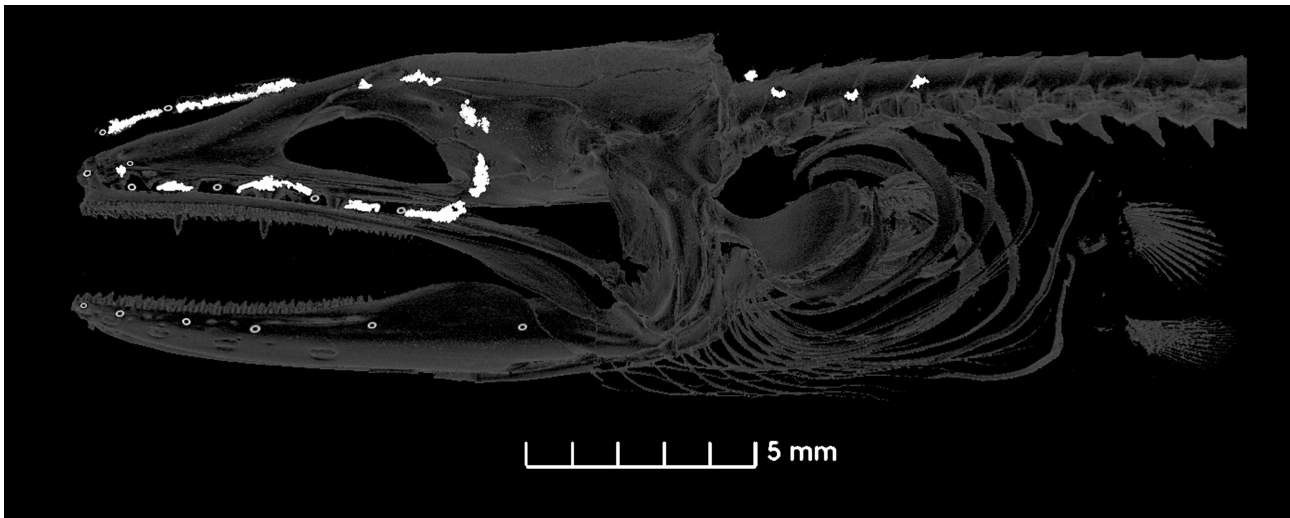


**FIGURE 8.** MicroCT scan of the anterior portion of holotype of *Dysommia pygmaea*, NMV A 29681-004 showing the left cephalic and lateral-line ossicles (white blotch-like areas) with associated pores.

Cephalic lateralis (Fig. 8). There are 11 cephalic-lateralis ossicles on the dorsal surface of the head, posterior to the eye and along the upper jaw. The anteriormost on the dorsal surface is associated with supraorbital lateralis pores 2 and 3. The next on the dorsal surface is the nasal ossicle which supports the dorsal portion of the nasal chamber. There are two very small ossicles along the portion of the supraorbital canal above the eye and two ossicles on the postocular portion of the infraorbital canal, but there are no pores associated with them. There are five ossicles associated with the infraorbital canal. The first, anterior most is on the adnasal branch of the infraorbital and the adnasal pore is near its distal end. The first infraorbital pore is anterior to the next infraorbital ossicle, near the junction of the adnasal branch with the main infraorbital canal. The second infraorbital pore is between the second and third infraorbital ossicles. The third infraorbital pore is posterior to the third infraorbital ossicle and the final infraorbital pore is anterior to the fifth infraorbital ossicle. Despite the lack of lateral line pores, there are 4–5 very small lateral-line ossicles in the dorsal branchial region posterior to the skull. These are probably vestigial but may still support the anterior portion of the lateralis nerve as there are superficial sensory papillae along the region of the lateral line despite the lack of open pores.

Neurocranium (Fig. 9). The skull of *D. pygmaea* is completely ossified with little cartilage and shows a generalized anguilliform pattern with the fused ethmovomer. The frontals are fused and cover nearly half of the dorsal surface of the skull. The remainder of the dorsal surface of the skull is composed of the paired parietals, pterotics, epiotics, sphenotics and the single, median supraoccipital. The ventral portion of the skull is composed of the fused ethmovomer, the parasphenoid, the prootics, the exoccipitals and the basioccipital. In addition, the lateral portions of the pterosphonoids, pterootics and sphenotics are visible in the ventral view. The dorsal portion of the orbit is formed primarily by the frontal. The ethmovomer forms the anterior margin of the orbit while the ventral and posterior margins are formed primarily by the parasphenoid. Robins and Robins (1970) reported that the basisphenoid and parasphenoid are fused in *D. rugosa*, but this could not be confirmed in *D. pygmaea* as there was no autogenous basisphenoid visible on the scan. The lack of an autogenous basisphenoid is not unique to *D. rugosa* and *D. pygmaea* as Robins and Robins (1970) also reported that the basisphenoid and parasphenoid are fused in *Dysomma anguillare*.



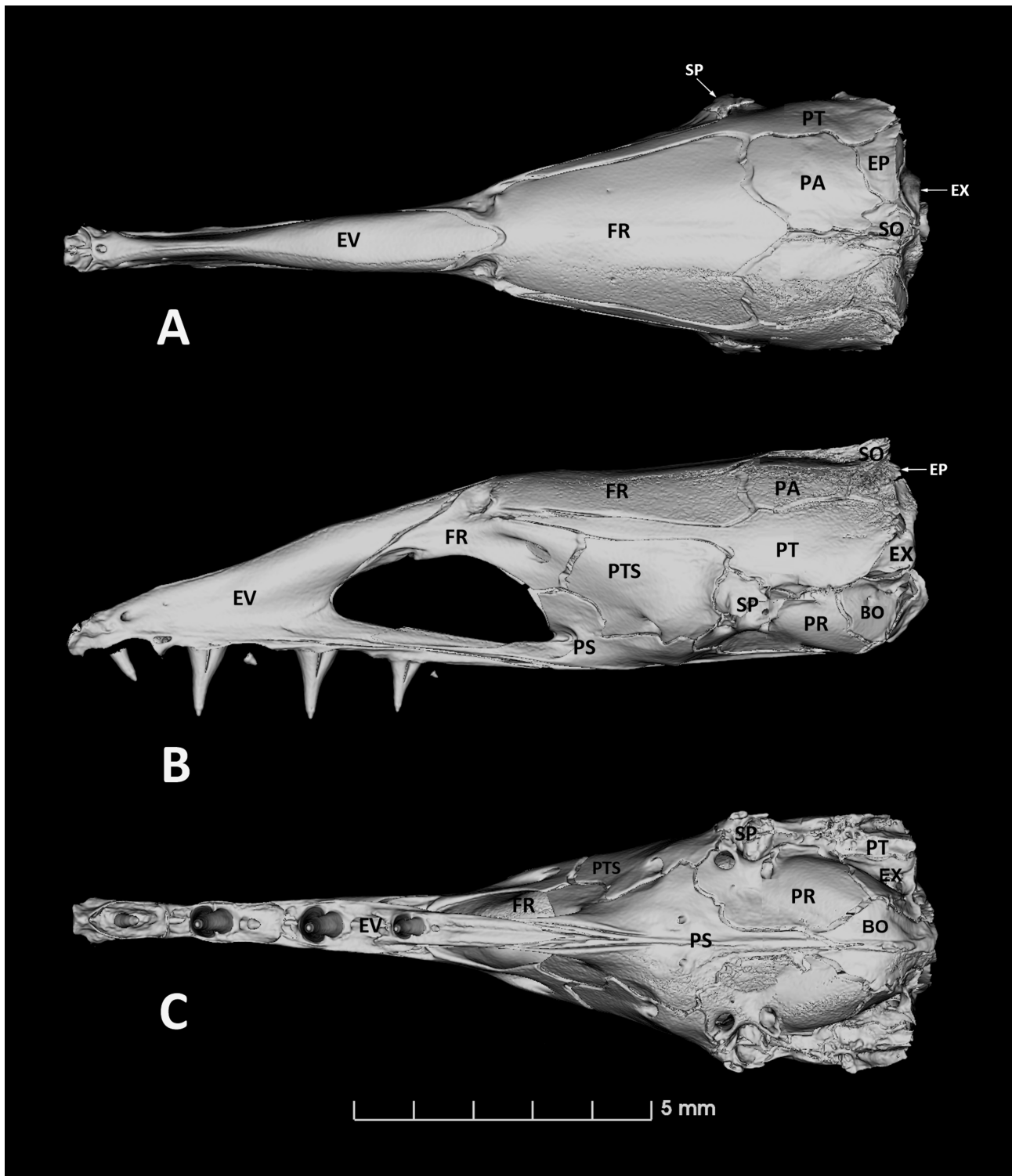


**FIGURE 9.** MicroCT scan of the neurocranium of holotype of *Dysommima pygmaea*, NMV A 29681-004. A. Dorsal view. B. Lateral view. C. Ventral view. Abbreviations: BO, basioccipital; EP, epiotic; EV, Ethmovomerine complex; EX, exoccipital; FR, frontal; PA, parietal; PR, prootic; PS, parasphenoid; PTS, pterosphenoid PT, pterotic; SO, supraoccipital; SP, sphenotic.

Suspensorium (Fig. 10). The hyomandibular is inclined slightly posteriorly and articulates with the neurocranium anteriorly with a hemispherical “ball and socket” joint underneath the sphenotic and posteriorly in a groove along the ventral surface of the pterotic. The hyomandibular and quadrate articulate in a complex interdigitated suture with a long triangular process of the hyomandibular extending nearly to the articulation of the quadrate with the

articular. The pterygoid is relatively stout but does not articulate the hyomandibular or quadrate. It is embedded within connective tissue or muscle and extends to near the posterior end of the maxilla. The opercular series is complete with all four elements present although greatly reduced in ossification especially along the margins. The opercle articulates with the hyomandibular through a bottle-neck articular condyle. The subopercle has an anterior arm that does not appear to articulate with any other bone of the opercular series. It becomes more laterally flattened posteriorly and curves around the ventral margin of the opercle. The preopercle lies along the posterior margin of the hyomandibular and is slightly tube-like to house the preopercular branch of the cephalic lateralis. The interopercle is a quadrilateral-shaped bone that is ventral and medial to the rest of the opercular series.

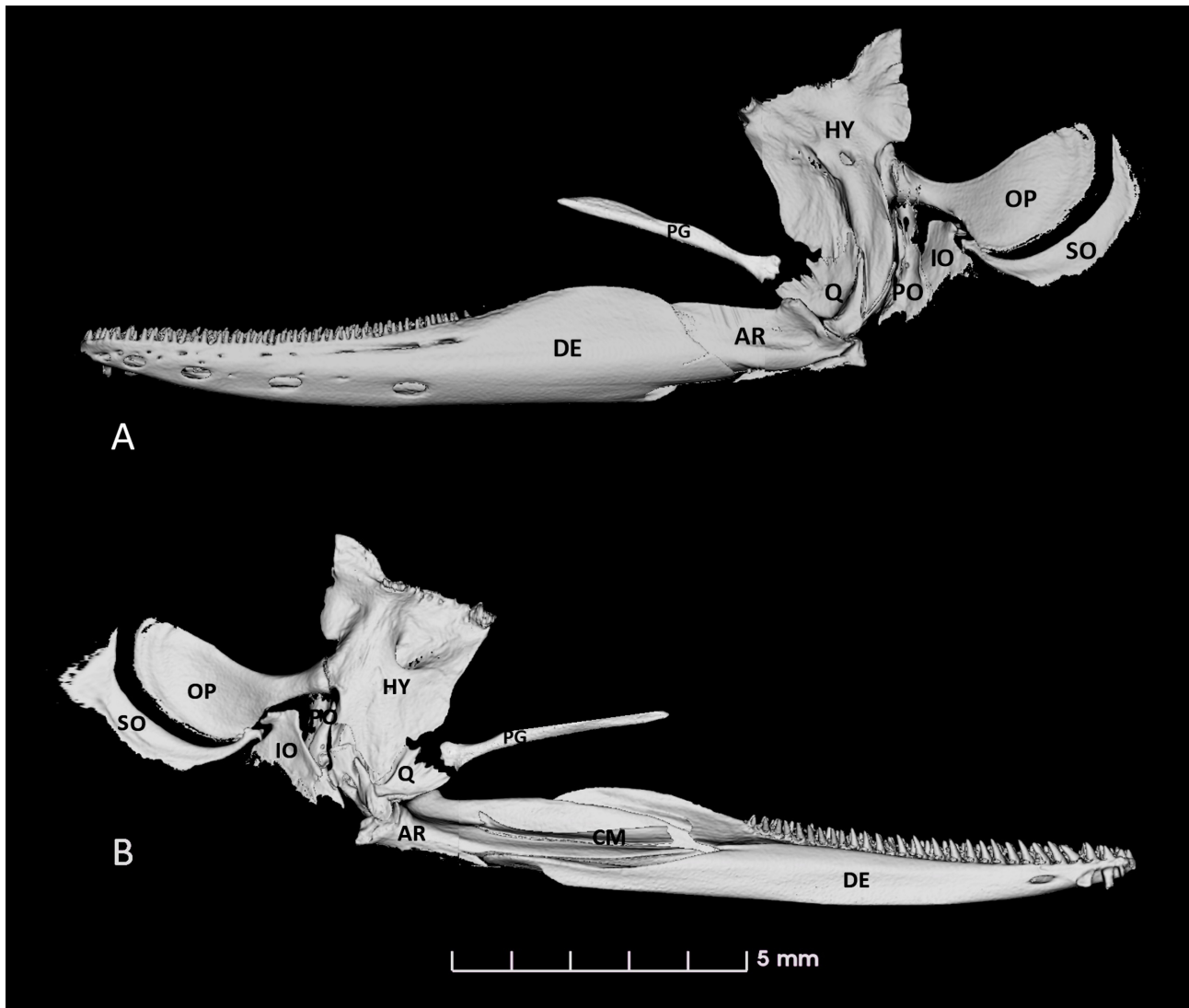


**FIGURE 10.** MicroCT scan of the left suspensorium, opercular series and lower jaw of holotype of *Dysommia pygmaea*, NMV A 29681-004. Lateral view. Abbreviations: AR, articular; CM, coronomeckelian ossification; DE, dentary; HY, hyomandibular; IO, interopercle; OP, opercle; PG, pterygoid; PO, preopercle; Q, quadrate; SO, subopercle.

Hyoid arch (Fig. 11). A median basihyal is present with paired hypohyals, anterior ceratohyals and posterior ceratohyals. The hypohyals are small cylindrical bones with a small ventral flange and are articulated to the anterior tip of the anterior ceratohyals. The anterior ceratohyals are also cylindrical with a narrow splint of bone extending onto the dorsal surface of the posterior ceratohyals. The posterior ceratohyals are cylindrical anteriorly but become laterally flattened and curve dorsally posteriorly. There are 12–13 branchiostegal rays (14 on the right arch of the holotype). The first originates at the end of the anterior ceratohyal, the second on the interspace between the anterior and posterior ceratohyals and the rest on the posterior ceratohyal. The last two are laterally flattened and curve up and around the opercle posteriorly, with the last ray nearly closing a circle.

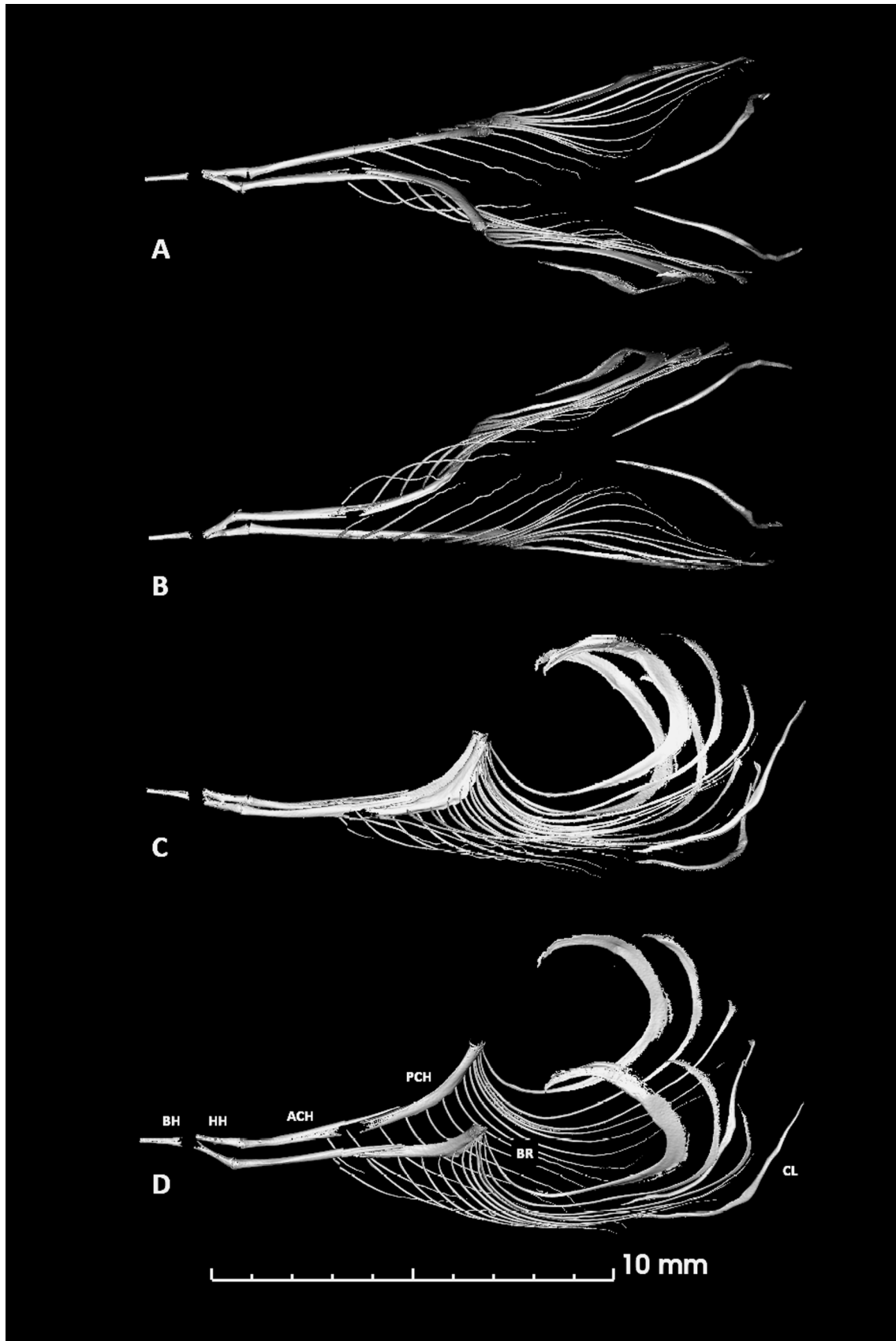


**FIGURE 11.** MicroCT scan of the hyoid arches of holotype of *Dysommima pygmaea*, NMV A 29681-004. A. Dorsal view. B. Ventral view. C. Lateral view. D. Dorso-lateral view. Abbreviations: ACH, anterior ceratohyal; BH, basihyal; BR, branchiostegal rays; CL, cleithrum; HH, hypohyal; PCH, posterior ceratohyal.

Pectoral fin (Fig. 12). The CT scan of the pectoral girdle shows the following elements: cleithrum, coracoid, four actinosts and 13 fin rays. The range of pectoral-ray counts from both scanned specimens and the cleared and stained specimen is 13–15 rays. Examination of the cleared and stained specimen also showed a lightly stained cartilaginous element just dorsal to the coracoid which is probably the scapula. Because of the cartilaginous nature of this element, it did not show up in the CT scans.

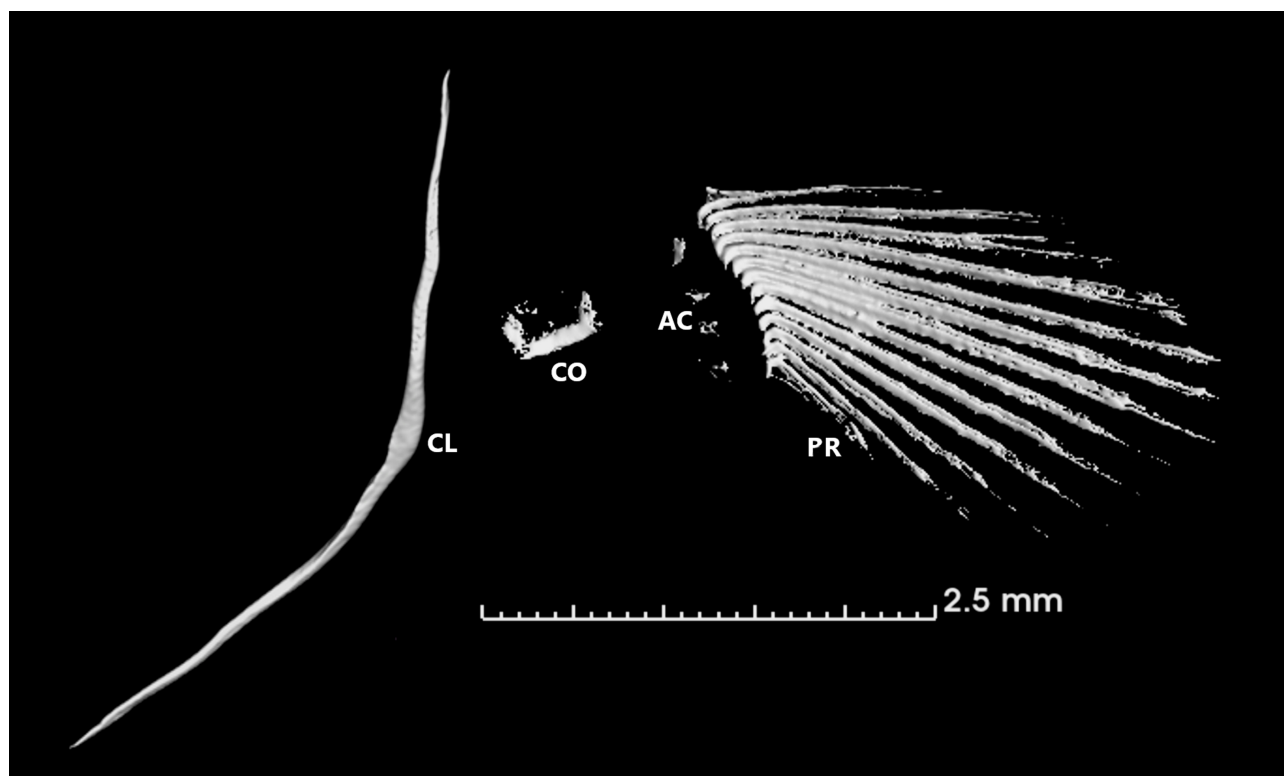


**FIGURE 12.** MicroCT scan of the left pectoral fin of holotype of *Dysommima pygmaea*, NMV A 29681-004. Lateral view. Abbreviations: AC, actinosts; CL, cleithrum; CO, coracoid; PR, pectoral rays.

Branchial arches (Fig. 13). Bones of the gill arches are the following: one unpaired median basibranchial, two pairs of hypobranchials, five pairs of ceratobranchials, four pairs of epibranchials, one pair of infrapharyngobranchials and two pairs of pharyngobranchial toothplates. Both lower and upper pharyngobranchial toothplates are roughly ovoid and covered with small, conical teeth. Robins and Robins (1970) reported that, in *D. rugosa*, there were two pairs of infrapharyngobranchials and that both lower and upper pharyngobranchial toothplates are single bones. In *D. pygmaea*, there is only a single pair of infrapharyngobranchials. In addition, the upper pharyngobranchial toothplates consist of two bones. The main bone of the toothplate is the upper pharyngobranchial 4 which is the largest and completely toothed. Anterior to this bone is a small elongate, sub-triangular bone (upper pharyngobranchial 3) which is closely associated (and possibly partially fused) with infrapharyngobranchial 3. Evidence that this is part of the upper pharyngobranchial toothplate is shown in Fig. 13D which shows a single tooth on the right upper pharyngobranchial 3 of USNM 443847.

**Comparative remarks.** *Dysommima pygmaea* can be distinguished from all other described species in the genus by its low vertebral count (122 versus 123–132 in *D. rugosa*, 137–141 in *D. orientalis*, and 133–134 in *D. brevis*) and higher predorsal vertebral count (16 versus 13–15 in *D. rugosa*, 11–12 in *D. orientalis*, and 12–13 in *D. brevis*). *D. pygmaea* also has a lower dorsal-ray count anterior to the anal-fin origin (29–34 versus 36–57 in *D. rugosa*, 51–60 in *D. orientalis*, and 41–42 in *D. brevis*). The coloration of *D. pygmaea* upon preservation is light tan overall with no dark pigmentation posteriorly on the anal base, anal fin, or caudal fin. All other species in the genus *Dysommima* are reported to have dark pigment somewhere posteriorly on the anal fin or caudal fin. In addition, the holotype and two of the paratypes of *D. pygmaea* are fully adult at a much smaller size than any other species in the genus. Maximum known size for *D. pygmaea* is 17 cm TL vs 32 cm TL for *D. brevis*, 35 cm TL for *D. rugosa* and 63 cm SL for *D. orientalis*.

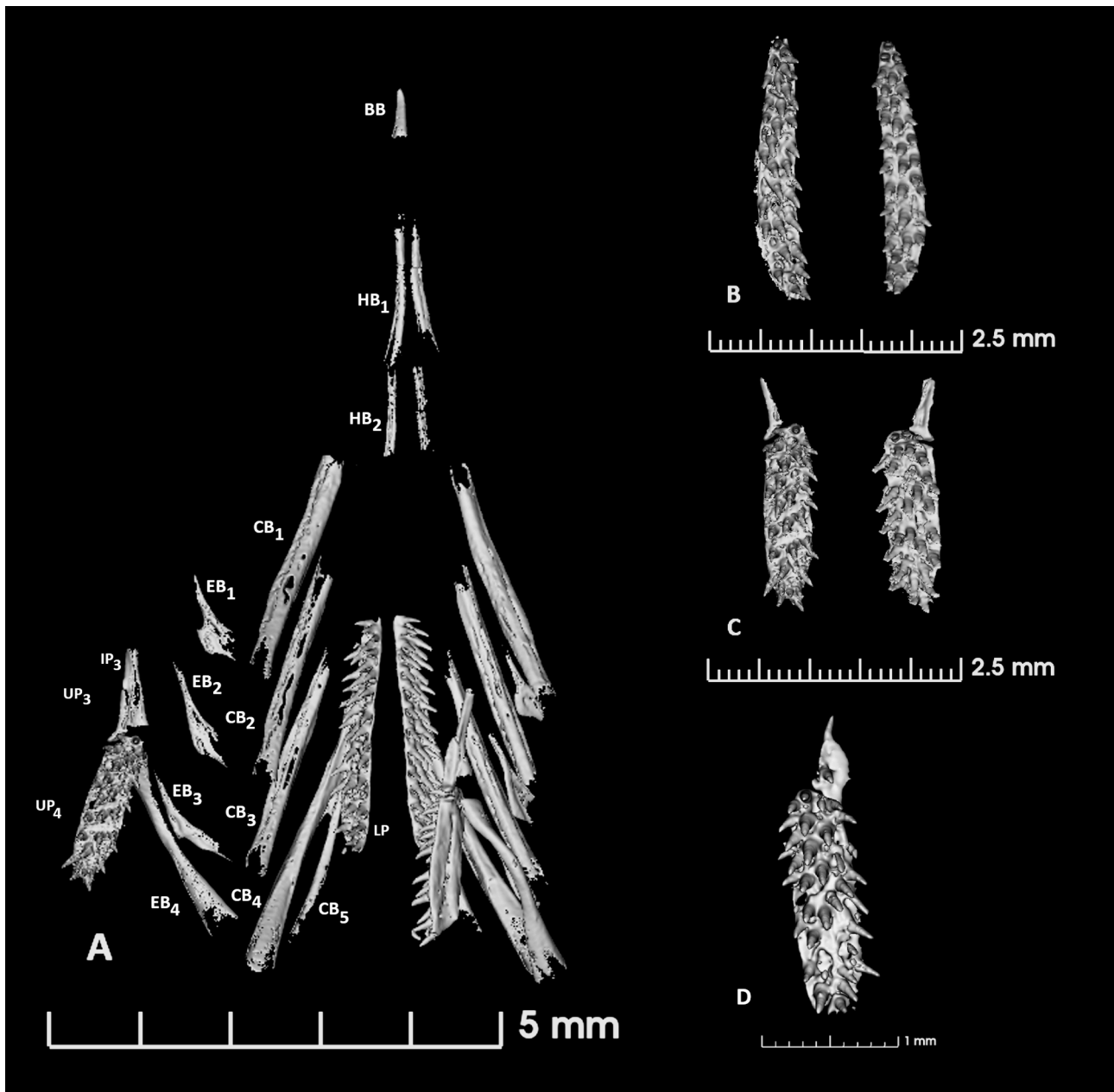


**FIGURE 13.** MicroCT scan of the branchial arches of *Dysommima pygmaea*, A. NMV A 29681-004. branchial arches in dorsal view, with upper elements of left branchial arch flipped to allow ventral view. B. NMV A 29681-004. lower pharyngeal toothplates. C. NMV A 29681-004. upper pharyngeal toothplates. D. USNM 443847, upper right pharyngeal toothplate. Abbreviations: BB, basibranchial; CB, ceratobranchial; EB, epibranchial; HB, hyobranchial; IP, infrapharyngobranchial; LP, lower pharyngeal toothplate; UP, Upper pharyngeal toothplate.

**Etymology.** The specific name *pygmaea* is the feminized form of the Latin noun *pygmaeus* meaning “dwarf” and refers to the small adult size of this species. A noun in apposition.

**Ecology.** The types were collected with a beam trawl deployed into a strong current. The beam trawl was successfully retrieved after a minor hookup on the rocky bottom with a good catch returned including some hard bottomed animals (glass sponges and stalked crinoids). Benthic fish genera collected with the types included *Chlorophthalmus*, *Hymenocephalus*, *Setarches* and *Symphurus*. Ross and Quattrini (2007), Ross *et al.* (2015a) and Ross *et al.* (2015b) reported the *Dysommima rugosa* was found primarily in complex, hard-bottomed habitats including rock fields, canyon walls, mixed hard-soft bottom, seeps and deep-water coral reefs. It is likely that *D. pygmaea* also inhabits similar habitats.



**Distribution.** *Dysommia pygmaea* is known only from the four specimens that were collected at a single trawl station near Rowley Shoals off Western Australia. The species is almost certainly more widely distributed in the eastern Indian Ocean but may remain rare in collections due to its rugged habitat which is difficult to sample.

**Comparative materials.** *Dysommia rugosa* (n=64): USNM 131594 (holotype, 196 mm TL), Atlantic Ocean, United States, Georgia, off Cumberland Island, 30°53'00"N, 79°42'30"W, 273 fms (499 m), 5 May 1886. USNM 44324 (1, 283 mm TL), Atlantic Ocean, United States, Georgia, off Savannah, 31°09'00"N, 79°33'30"W, 644 m, 5 May 1886. USNM 179213 (1, 194 mm TL), Gulf of Mexico, off Florida, 28°16'N, 85°50'W, 439 m, 3 Dec 1962. USNM 190541 (1, 265 mm TL), Gulf of Mexico, Florida Keys, southwest of Dry Tortugas, 24°28'N, 83°24'W, 329 m, 7 Jun 1959. USNM 193552 (1, 213 mm TL), Caribbean Sea, off Belize, 16°58'N, 87°53'W, 250–400 fms (457–732 m), 10 Jun 1962. USNM 200776 (1, 248 mm TL), Atlantic Ocean, east coast of Florida, 29°59'N, 80°09'W, 347 m, 21 Nov. 1965. USNM 441960 (1, 226 mm TL), USNM 441961 (1, 224 mm TL), Atlantic Ocean, off Maryland, Baltimore Canyon seep, 38°02'53"N, 73°49'19"W, 398 m, 16 May 2013. USNM 441962 (1, 249 mm TL), Atlantic Ocean, off Maryland, Baltimore Canyon seep, 38°02'57.1"N, 73°49'19.6"W, 414 m, 7 Sep 2012. NCSM 115346 (1, 96 mm TL), Atlantic Ocean, off North Carolina, Cape Lookout Lophelia A, ca. 197.3–197.6 kilometers E of Wilmington, 34°19'42"N, 75°47'59"W, 370–407 m, 15 Jun 2004. NCSM 115347 (1, 180 mm TL), Atlantic Ocean, off North Carolina, Cape Lookout Lophelia B, ca. 90.6–91.2 kilometers SE of Beaufort, 34°13'55"N, 75°52'01"W, 419–430 m, 20 Sep 2006. NCSM 115348 (2, 128–157 mm TL), Atlantic Ocean, off North Carolina, Lophelia B site, ca. 75.7 kilometers SE Cape Lookout, 34°10'50"N, 75°53'28"W, 397–450 m, 19 Oct 2005. NCSM 115349 (1, 174 mm TL), Atlantic Ocean, off North Carolina, Cape Lookout Lophelia B, ca. 92.9–93.6 kilometers SE of Beaufort, 34°10'54"N, 75°52'57"W, 458–465 m, 19 Sep 2006. NCSM 115350 (1, 176 mm TL), Atlantic Ocean, off North Carolina, Cape Lookout Lophelia A, ca. 92.4–92.3 kilometers ESE of Beaufort, 34°18'48"N, 75°47'4"W, 389–443 m, 23 Sep 2001. NCSM 115351 (1, 184 mm TL), Atlantic Ocean, off North Carolina, Cape Lookout Lophelia A, ca. 91.2 kilometers ESE of Beaufort, 34°19'25"N, 75°47'30"W, 367–399 m, 22 Sep 2001. NCSM 115352 (4, 80–158 mm TL), Atlantic Ocean, off North Carolina ca. 74.7–75.1 kilometers SE of Cape Lookout, 34°11'12"N, 75°53'49"W, 431 m, 19 Sep 2006. NCSM 115353 (1, 193 mm TL), Atlantic Ocean, off Maryland, Baltimore Canyon, ca. 115.7–117.9 kilometers ESE of Ocean City, 38°02'47"N, 73°49'07"W, , 7 Sep 2012. NCSM 115354 (3, 145–217 mm TL), Atlantic Ocean, off North Carolina, Cape Lookout Lophelia B, ca. 92.8–92.9 kilometers SE of Beaufort, 34°10'46"N, 75°53'26"W, 450–487 m, 24 Sep 2001. NCSM 115355 (2, 220–225 mm TL), Atlantic Ocean, off Maryland, Baltimore Canyon, ca. 159.6–159.2 kilometers ESE of Salisbury, 38°02'52"N, 73°49'11"W, 399–443 m, 16 May 2013. NCSM 115356 (1, 210 mm TL), Atlantic Ocean, off North Carolina, Cape Lookout Lophelia A, ca. 90.7–90.3 kilometers ESE of Beaufort, 34°19'06"N, 75°48'13"W, 396–405 m, 10 Aug 2002. NCSM 115357 (15, 166–206 mm TL), Atlantic Ocean, off North Carolina, Cape Lookout Lophelia B, ca. 91.7–92.3 kilometers SE of Beaufort, 34°11'57"N, 75°52'59"W, 423–443 m, 19 Sep 2006. NCSM 115358 (4, 169–237 mm TL), Atlantic Ocean, off North Carolina, Cape Lookout, ca. 91.8–91.7 kilometers ESE of Beaufort, 34°17'38"N, 75°48'19"W, 438–439 m, 5 Dec 2009. ANSP 94286 (1, 155 mm TL), Atlantic Ocean, off St. Augustine, 29°56'N, 80°10'W, M/V Combat sta. 84, 190 fms (165 m), 1 September 1956. ANSP 102469 (1, 162 mm TL), Atlantic Ocean, Atlantic coast of Florida, 29°53'N, 80°11'W, R/V Silver Bay sta. 3677, 180 fms (329 m), 20 January 1962. ANSP 106150 (1, 149 mm TL), Atlantic Ocean, Atlantic coast of Florida, 30°21'N, 79°55'W, 230–250 fms (420–457 m), R/V Atlantis sta. 3779, 24 February 1940. ANSP 110079 (1, 337 mm TL), Atlantic Ocean, Atlantic coast of Florida, 92°53'N, 80°11'W, 175–180 fms (320–329 m), R/V Silver Bay sta. 3669, 18 January 1962. ANSP 114438 (1, 245 mm TL), Atlantic Ocean, Gulf of Mexico, Straits of Florida, 24°26'N, 83°31'W, 300 fms (549 m), R/V Oregon sta. 4373, 7 August 1963. ANSP 114439 (1, 218 mm TL), Atlantic Ocean, between Florida and The Bahamas, 26°14'N, 79°30.5'W, 351 fms (642 m), R/V Gerda sta. 299, 5 April 1964. ANSP 114440 (1, 173 mm TL), Atlantic Ocean, Straits of Florida, 24°10'N, 81°39'W, 345 fms (631 m), R/V Gerda sta. 362, 15 September 1964. ANSP 114441 (1, 228 mm TL), Atlantic Ocean, Atlantic coast of Florida, 157–143 fms (287–262 m), R/V Gerda sta. 655, 16 July 1965. ANSP 114442 (1, 174 mm TL), Atlantic Ocean, Atlantic coast of Florida, 27°08'N, 79°45'W, 220 fms (403 m), R/V Gerda sta. 652, 16 July 1965. ANSP 114443 (1, 166 mm TL), Atlantic Ocean, Atlantic coast of Florida, 29°55'N, 80°11'W, 180–182 fms (329–333 m), R/V Silver Bay sta. 3675, 19 January 1962. ANSP 114444 (1, 338 mm TL), Atlantic Ocean, Atlantic coast of Florida, 29°53'N, 80°11'W, 180 fms (329 m), R/V Silver Bay sta. 3680, 21 January 1962. ANSP 114445 (1, 347 mm TL), Atlantic Ocean, Atlantic coast of Florida, 29°42'N, 80°11'W, 170 fms (311 m), R/V Silver Bay sta. 3679, 20 January 1962. ANSP 114449 (1, 137 mm TL), Atlantic Ocean, Atlantic coast of Florida, 30°40'N, 79°57'W, 210 fms (384 m), M/V Combat sta. 310, 24 April 1957. ANSP 117045 (1, ca. 280 mm TL), Atlantic Ocean, off Florida, 30°2'N, 80°6'W, 215 fms (393 m), R/V Oregon sta 5761, 20 November

1965. ANSP 130216 (1, 268 mm TL), Atlantic Ocean, off coast of North Carolina, 33°56'N, 75°56'W, 340 fms (622 m), R/V Oregon sta. 11758, 31 January 1972. ANSP 130217 (1, 175 mm TL), Atlantic Ocean, off Florida, 30°54'N, 79°40'W, 265 fms (485 m), R/V Oregon sta 11715, 21 January 1972. ANSP 130219 (1, 211 mm TL), Atlantic Ocean, off Georgia, 31°2'N, 79°48'W, 140 fms (256 m), R/V Oregon sta 11710, 20 January 1972. ANSP 153725 (1, 269 mm TL), Atlantic Ocean, Straits of Florida, 24°27'N, 83°25'W, 200 fms (366 m), R/V Oregon sta 11166, 17 August 1970.

*Dysommia orientalis* (n=7): NMMB-P11131 (holotype, 413 mm TL), collected from Dong-gang fishing port, Pingtung, Taiwan, 13 Sep. 2010. USNM 441667 (paratype, 316 mm TL; formerly NMMB-P14012), Dong-gang fishing port, Pingtung, Taiwan, 20 Oct. 2011; NMMB-P3847 (paratype, 290 mm TL; formerly THUP 4077), Dong-gang fishing port, Pingtung, Taiwan, 21 Mar. 1979; NMMB-P8361 (paratype, 258 mm TL), Dong-gang fishing port, Pingtung, Taiwan, 16 Mar. 2005; USNM 441750 (paratype, 325 mm TL; formerly NSYSU 3028), Dong-gang fishing port, Pingtung, Taiwan, Jan. 1996; ASIZP 57954 (paratype, 238 mm TL), Dong-sha Island, South China Sea, 17 Aug. 1991; OMNH-P10000 (paratype, 625 mm TL), Suruga Bay, Shizuoka Prefecture, Japan, 34°54'N, 138°30.5'E, 300–400 m depth, 17 Dec. 1996.

## Acknowledgements

The authors wish to thank Martin F. Gomon who collected the type series and provided the photograph of the holotype. We also wish to thank Dianne J. Bray for the loan of the specimens and gifting of one paratype to the National Museum of Natural History (USNM), and Alastair Graham (CSIRO) for facilitating the loan and registration of specimens. We thank Carlie Devine (CSIRO) for photography of the preserved holotype and Emily Gumina (CSIRO) for image etching and manipulation. We also thank the staff of the North Carolina Museum of Natural Sciences and the Academy of Natural Sciences of Drexel University for allowing the senior author to examine specimens that are under their care. The senior author would also like to thank Matthew G. Girard and Leo MacLeod for their help with the microCT scanner and 3D Slicer.

## References

- Böhlke, E.B. (1982) Vertebral formulae for type specimens of eels (Pisces: Anguilliformes). *Proceedings of the Academy of Natural Sciences, Philadelphia*, 134, 31–49.
- Böhlke, E.B. (1989) Methods and terminology. In: Böhlke, E.B. (Ed.), *Fishes of the Western North Atlantic. Memoir of the Sears Foundation for Marine Research*, 1 (Part 9), pp. 1–7.
- Chen, Y.-Y. & Mok, H.-K. (2001) A new synphobranchid eel, *Dysomma longirostrum* (Anguilliformes: Synphobranchidae), from the northeastern coast of Taiwan. *Zoological Studies*, 40 (2), 79–83.
- Fedorov, A., Beichel, R., Kalpathy-Cramer, J., Finet, J., Fillion-Robin, J.-C., Pujol, S., Bauer, C., Jennings, D., Fennessy, F., Sonka, M., Buatti, J., Aylward, S., Miller, J.V., Pieper, S. & Kikinis, R. (2012) 3D slicer as an image computing platform for the quantitative imaging network. *Magnetic Resonance Imaging*, 30, 1323–1341.  
<https://doi.org/10.1016/j.mri.2012.05.001>
- Ginsburg, I. (1951) The eels of the northern Gulf Coast of the United States and some related species. *Texas Journal of Science*, 3 (3), 431–485.
- Haimovici, M., Martins, A.S., Figueredo, J.L. & Viera, P.C. (1994) Demersal bony fish of the outer shelf and upper slope of the southern Brazil Subtropical Convergence Ecosystem. *Marine Ecology Progress Series*, 108, 59–77.  
<https://doi.org/10.3354/meps108059>
- Hatooka, K. (1997) First record of the deep-sea eel, *Dysommia rugosa* from Suruga Bay, Central Japan (Pisces: Synphobranchidae). *Bulletin of the Osaka Museum of Natural History*, 51, 7–12.
- Ho, H.-C., Smith, D.G. & Tighe, K.A. (2015) Review of the arrowtooth eel genera *Dysomma* and *Dysommia* in Taiwan, with the description of a new species (Anguilliformes: Synphobranchidae: Ilyophinae). *Zootaxa*, 4060 (1), 86–104.  
<https://doi.org/10.11646/zootaxa.4060.1.12>
- Karrer, C. (1983) Anguilliformes du Canal de Mozambique (Pisces, Teleostei). *Faune Tropicale*, 23, 1–116.
- Robins, C.H. & Robins, C.R. (1970) The eel family Dysommidae (including the Dysommidae and Nettodaridae), its osteology and composition, including a new genus and species. *Proceedings of the Academy of Natural Sciences of Philadelphia*, 122 (6), 293–335.
- Robins, C.H. & Robins, C.R. (1976) New genera and species of dysommine and synphobranchine eels (Synphobranchidae) with an analysis of the Dysommidae. *Proceedings of the Academy of Natural Sciences, Philadelphia*, 127 (18), 249–280.

- Robins, C.H. & Robins, C.R. (1989) Family Synphobranchidae, pp. 207–253. In: Böhlke, E.B. (Ed.), *Fishes of the Western North Atlantic. Memoir of the Sears Foundation for Marine Research*, 1 (Part 9), pp. 1–655.  
<https://doi.org/10.2307/j.ctvbc0dm.12>
- Ross, S.W. & Quattrini, A.M. (2007) The fish fauna associated with deep coral banks off the southeastern United States. *Deep Sea Research Part I Oceanographic Research Papers*, 54, 975–1007.  
<https://doi.org/10.1016/j.dsr.2007.03.010>
- Ross, S.W., Brooke, S., Quattrini, A.M., Rohde, M. & Watterson, J.C. (2015a) A deep-sea community, including *Lophelia pertusa*, at unusually shallow depths in the western North Atlantic Ocean off northeastern Florida. *Marine Biology*, 162, 635–648.  
<https://doi.org/10.1007/s00227-015-2611-2>
- Ross, S.W., Rohde, M. & Quattrini, A.M. (2015b) Demersal fish distribution and habitat use within and near Baltimore and Norfolk Canyons, U.S. middle Atlantic slope. *Deep Sea Research Part I Oceanographic Research Papers*, 103, 137–154.  
<https://doi.org/10.1016/j.dsr.2015.06.004>
- Sabaj, M.H. (2020) Codes for Natural History Collections in Ichthyology and Herpetology. *Copeia*, 108 (3), 593–669.  
<https://doi.org/10.1643/ASIHCONDONS2020>
- Sabaj, M.H. (2025) *Codes for Natural History Collections in Ichthyology and Herpetology (online supplement). Version 9.7. 3 March 2025*. American Society of Ichthyologists and Herpetologists, Washington, D.C. Available from: <https://www.asih.org/resources/standard-symbolic-codes> (accessed 1 May 2025)
- Saruwatari, T., López, J.A. & Pietsch, T.W. (1997) Cyanine Blue: a versatile and harmless stain for specimen observation. *Copeia*, 1997 (4), 840–841.  
<https://doi.org/10.2307/1447302>
- Staudigel, H., Hart, S.R., Pile, A., Biale, B.E., Baker, E.T., Brooke, S., Connelly, D.P., Haucke, L., German, C.R., Hudson, I., Jones, D., Koopers, A.A.P., Konter, J., Lee, R., Pietsch, T.W., Tebo, B.M., Templeton, A.S., Zierenberg, R. & Young, C.M. (2006) Vailulu'u Seamount, Samoa: Life and death on an active submarine volcano. *Proceedings of the National Academy of Sciences*, 103 (17), 6448–6453.  
<https://doi.org/10.1073/pnas.0600830103>
- Tighe, K.A., Ho, H.-C. & Hatooka, K. (2018) A new species of the genus *Dysommia* (Teleostei: Anguilliformes: Synphobranchidae: Ilyophinae) from the Western Pacific. *Zootaxa*, 4454 (1), 43–51.  
<https://doi.org/10.11646/zootaxa.4454.1.6>
- Tweddle, D. & Anderson, M.E. (2008) A collection of marine fishes from Angola, with notes on new distribution records. *Smithiana Bulletin*, 8, 3–24.
- Uyeno, T. & Sasaki, K. (1983) *Dysommia rugosa* Ginsburg, 1951. In: Uyeno, T., Matsubara, T. & Fuji, E. (Eds.), *Fishes trawled off Surinam and French Guiana*. Japan Marine Fishery Resource Research Center, Tokyo, pp. 1–107.
- Vo, Q.V., Ho, H.-C., Dao, H.V. & Tran, T.C. (2024) New species of the eel genera *Dysomma* and *Dysommia* from Vietnam, South China Sea (Anguilliformes: Synphobranchidae). *Journal of Fish Biology*, 104 (4), 1067–1078.  
<https://doi.org/10.1111/jfb.15638>